Full Length Research Paper

Bond length effect of fiber reinforced polymers bonded reinforced concrete beams

Y. Sümer[1]* and M. Aktaş[2]

Civil Engineering Department, Faculty of Engineering, Sakarya University, Turkey.

There has been a large amount of experimental study on strengthening of concrete structures in recent years. An alternative method to experimental study is the finite element method when studying the performance of concrete beams strengthened with fiber reinforced polymer. Although many improvements have been recorded with the experimental studies, there are still needs for reliable numerical studies. The behavior of the complete composite system with concrete, adhesive, fiber reinforced polymer, and internal reinforcement is quite complex. In this study, two-dimensional nonlinear finite element model is developed. The framework of damage mechanics is used during the finite element modeling. Nonlinear material behavior, as it relates to steel reinforcing bars, concrete, epoxy and fiber reinforced polymer is simulated using appropriate constitutive models. Finite element model is verified by two different experimental studies by employing commercial finite element software package, Abaqus. Since comparisons between the numerical and experimental results show very good agreement in terms of the load-deflection, load-strain relationships, the particular emphasis is placed on the search of the effect of fiber reinforced polymer bond length on failure load of externally strengthened beams. The results of simulations indicate that, the change in bond length of fiber reinforced polymer through constant moment region has no effect on the ultimate load capacity of strengthened beams.

Key words: Finite element method, reinforced concrete beam, fiber reinforced polymer (FRP) bond length, concrete damaged plasticity, Abaqus.

INTRODUCTION

The use of externally bonded fiber reinforced polymer (FRP) composites has steadily increased as an efficient technique for structural rehabilitation of damaged or deficient concrete members in the last thirty years. These FRP materials are generally bonded externally to the tension face of concrete beams with any desirable shape via a thin layer of epoxy adhesive and thus enhance stiffness and strength of structural members. The macro response of FRP-strengthened beams has extensively been studied experimentally from the aspect of overall strengthening, ductility, and failure. However, effective application of FRP to concrete structure is possible after a fundamental understanding of the mechanisms of the retrofitted system.

Experimental studies are inevitable to provide necessary guidance in design, nevertheless laboratory testing is limited, took long times considering the member sizes, loading and support conditions, and moreover it is not cost effective. Nonlinear finite element analysis can provide a powerful tool to study the behavior of concrete structures (Pham, and Al-Mahaidi, 2005) and very important to conduct researches for further investigations. One of the first analytical works on the behavior of FRP-strengthened beams is that presented by Ehsani and Saadatmanesh (1990). This is based on linear elastic analyses and obtained numerical result is stiffer than the experimental results. Malek and Saadatmanesh (1998) proposed an analytical model to simulate concrete and steel reinforcement. They modeled FRP composites by neglecting the bond slip behavior between FRP and concrete. More realistic numerical models, including the material nonlinearities of the concrete are developed by

---

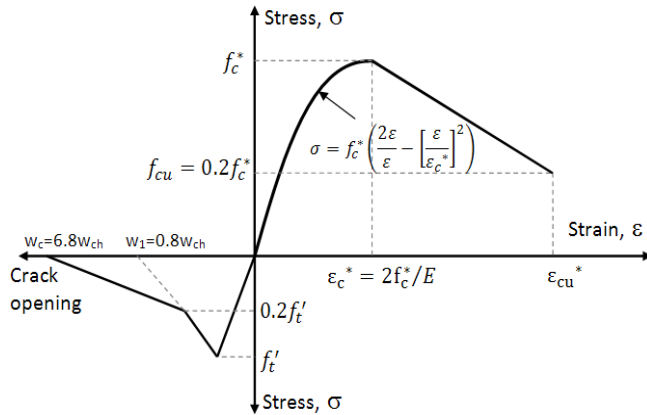*Corresponding author. E-mail: yusufsumer@gmail.com.

Figure 1. Constitutive law for concrete.

Table 1. Aggregate size-based fracture coefficients (Rots, 1988).

Maximum agregate size, d_{max} (mm)	Coefficient , G_{fo}, (J/m^2)
8	25
16	30
32	58

other researchers (Takahashi et al., 1997; Nitereka and Neale, 1999). Yang et al. (2001) and Ebead et al. (2004) modeled the adhesive layer as a linear elastic material, rather than full bond assumption as commonly used. Yang et al. (2003) presented a finite element model (FEM) based on linear elastic fracture mechanics approach that has very complicated remeshing process to simulate the concrete cracking with no consideration of the tension softening behavior. Niu et al. (2006) and Baky et al. (2007) also studied different modeling approaches particularly interfacial response of FRP strengthened reinforced concrete (RC) beams. However these modeling techniques are not easy to implement even for simple applications.

This study aims to have an experimentally verified non-linear FEM of simply supported RC beam strengthened with FRP. The accuracy of the finite element modeling is assessed against two different published experimental data. Also the effect of FRP length on the ultimate load capacity of the strengthened RC beam is investigated by changing the length of the FRP. Subsequently, modeling strategies and the material models used in finite element model was described.

Finite element modeling approach

The fundamental step of creating FEM is to define the constitutive relationships of materials as realistic as possible to obtain the nonlinear behavior of the system. Concrete plays crucial role in this

study. Thus, plasticity based concrete constitutive model named Concrete Damage Plasticity (CDP) that utilizes the classical concepts of the theory of plasticity is used in this analysis.

Constitutive behaviors and material models for concrete, steel, FRP and epoxy

In general, the nonlinearity of concrete under compression can be modeled by approaches based on the concept of either damage or plasticity, or both (Yu et al., 2010). Plasticity is generally defined as the unrecoverable deformation after all loads have been removed. Damage is generally characterized by the reduction of elastic stiffness. CDP model which combines the effect of damage and plasticity is used in this study. Two main failure mechanisms, tensile cracking and compressive crushing of the concrete, are assumed for CDP (Abaqus User Manual, 2009). The basic parameters required to implement this model are as follows: Dilation angle (ψ) that is measured in the p-q plane (p: hydrostatic pressure stress, which is a function of the first stress invariant, q: second deviatoric stress invariant) at high confining pressure and it is accepted 30° as recommended in the literature. ϵ, is an eccentricity of the plastic potential surface with default value of 0.1. The ratio of initial biaxial compressive yield stress to initial uniaxial compressive yield stress is defined by σ_{bo}/σ_{co}, with a default value of 1.16. Finally, K_c is the ratio of the second stress invariant on the tensile meridian to compressive meridian at initial yield with default value of 2/3 (Abaqus User Manual, 2009). The parameter K_c should be defined based on the full triaxial tests of concrete, moreover biaxial laboratory test is necessary to define the value of σ_{bo}/σ_{co}. This paper does not discuss the identification procedure for parameters ϵ, σ_{bo}/σ_{co}, and K_c because tests that are going to be verified in this study do not have such information. Thus, default values are accepted in this study. On the other hand, concrete compression and tension damage parameters are defined with the same method as in Sumer and Aktas (2010).

Since the compression and tension stress-strain relation of the test specimens are not reported in the test reports, these relations are created by using mathematical models from literature. Stress-strain curve of concrete under uniaxial compression is obtained by employing Hognestad parabola (Hognestad, 1951) along with linear descending branch. Some modifications are made to this parabola according to CEB-FIP MC90 (CEB-FIB, 1993) due to the affects of closed stirrups. Hence, stirrups are not modeled individually but their effects are included in the properties of concrete. A Figure 1 display a schematic representation of the uniaxial material response consistent with Equation (1) in which σ is the compressive stress, f_{cu} is the ultimate compressive stress, ϵ_c^* is the peak compressive strain, E is the elastic modulus and f_c^* is the modified compressive strength. More details about these modified values can be found in Arduni et al. (1997).

$$\sigma = f_c^* \left(\frac{2\epsilon}{\epsilon} - \left[\frac{\epsilon}{\epsilon_c^*} \right]^2 \right) \tag{1}$$

Concrete constitutive relation in tension is defined by bilinear model as seen in Figure 1 (Coronado and Lopez, 2006). When there is no reinforcement in significant regions of the model and cracking failure is not evenly distributed, mesh sensitivity problem exists. To overcome unreasonable mesh sensitivity problem Hillerborg' s et al. (1976) fracture energy approach is used instead of tensile strain and it is calculated as a ratio of the total external energy supply (G_F) per unit area required to create crack in concrete. In Equation (2), tensile fracture energy of concrete, (G_F), is defined as a function of concrete compressive strength, f_c^*, and a coefficient, G_{fo}, which is related to the maximum aggregate size (CEB-FIB 1993). Several values for G_{fo} is given in Table 1.
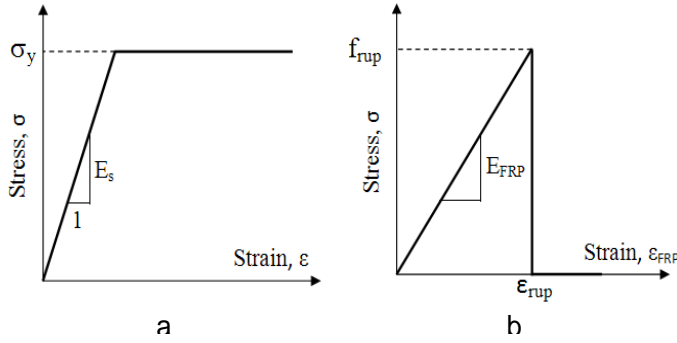
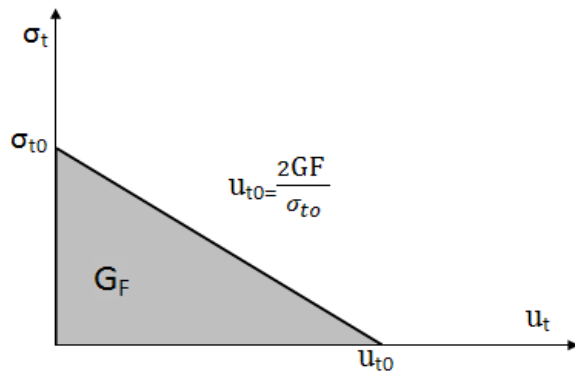**Figure 2.** Material models for (a) steel and (b) FRP composites.

Figure 3. Post failure stress-strain relation with fracture energy approach (Abaqus User Manual, 2009).
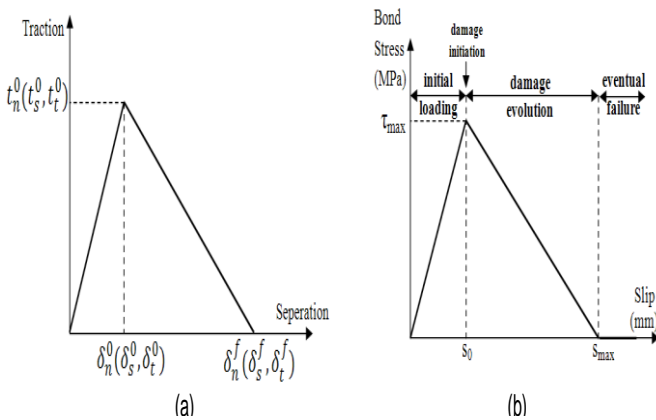

Figure 4. Traction-separation model for interface behavior.

$$G_F = G_{fo} \left(\frac{f_c^*}{10}\right)^{0.7} \qquad (2)$$

The stress–strain curve of the reinforcing bar is assumed to be elastic perfectly plastic as shown in Figure 2a. The parameters needed to specify this behavior are the modulus of elasticity (E_s), Poisson ratio (υ) and yield stress (f_y). However, in the literature, most studies of RC structures strengthened by FRP have assumed

the behavior of FRP to be linear. The behavior of FRP composites is predicted using a linear elastic material model. In this approach, the FRP behavior is assumed to be linear up to failure strain (ε_{rup}) is reached (Figure 2b).

Interface behavior between rebar and concrete is modeled by implementing tension stiffening in the concrete modeling to simulate load transfer across the cracks through the rebar. Tension stiffening also allows to model strain-softening behavior for cracked concrete. Thus, it is necessary to define tension stiffening in CDP model. Tension stiffening is modeled by applying a fracture energy cracking criterion. In this approach; the amount of energy (G_F) required to open a unit area of crack (u_{t0}) is assumed as a material property (Figure 3).

A bond-slip model is applied to interface elements to model the bond mechanism between FRP and concrete material. The constitutive behavior of interface elements is defined in terms of traction-separation behavior. Figure 4a displays a schematic representation of such behavior with what is used in the present work. This model includes initial loading, initiation of damage, and propagation of damage leading to eventual failure at the bonded interface (Abaqus User Manual, 2009). The material model of the FRP-concrete interface is simulated as a bond-slip relationship between local shear stress, τ, and the relative displacement, δ, at the interface. One of the most accurate bond stress–slip models that can be incorporated into a finite-element analysis is proposed by Lu et al. (2005). In their study, existing bond–slip models are assessed by using the results of 253 pull tests from literature. On the other hand, three different bond–slip models, the precise, the simplified, and the bilinear model; have been recommended by Lu et al. (2005). They suggest that bilinear model gives better results than the others do. Thus, in the current study, the bilinear model, as shown in Figure 4b is adopted.

In this model τ_{max} and s_0 are the maximum bond stress and corresponding slip, respectively. Ascending ($s \leq s_0$) and descending ($s > s_0$) part of this model are defined as in Table 2. In these equations, α_1 is a coefficient and it is recommended as 1.5 (Lu et al., 2005).

Geometrical modeling

After defining material models, geometry of the beam is modeled as plotted in Figure 5. For simplicity, stirrups are not considered as a geometrical entity but their effect is considered by introducing a confined concrete model for the RC beam element. The element types used for constructing the finite element models are listed in Table 3. Interaction between concrete, epoxy and FRP are achieved by the surface tie definition. Steel bars are embedded in concrete with the same degrees of freedom meaning that there is a perfect bond between concrete and steel. Concrete is modeled by using four-noded plain strain element with reduced integration formula. Since first order elements use linear interpolation to obtain nodal displacements, the edges of these elements are unable to curve under bending resulting in shear rather than bending deformation. This phenomenon is known as shear locking (Abaqus User Manual, 2009). Element with reduced integration formula is employed to overcome this problem. All the beams are loaded by displacement control in the vertical direction.

Since there is no computational expense, all the beams are modeled with full geometry in two dimensions.

VERIFICATION STUDY

Employing the aforementioned modeling strategies, the two FRP-strengthened flexural cases are reproduced and

Table 2. Definition of bilinear bond-slip model.

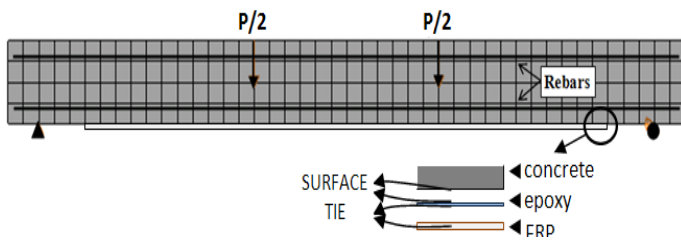| Equation	Current range
$\tau = \tau_{max} \dfrac{s}{s_o}$	$s \leq s_0$
$\tau = \tau_{max} \dfrac{s_f - s}{s_f - s_o}$	$s_0 \leq s \leq s_f$
$\tau = 0$	$s \geq s_f$
$s_f = \dfrac{2G_f}{\tau_{max}}$	$G_f = 0.308 \cdot \beta_w^2 \sqrt{f_t}$
$s_0 = 0.0195 \cdot \beta_w \cdot f_t$	$\beta_w = \sqrt{\dfrac{2 - b_f/b_c}{1 + b_f/b_c}}$
$\tau_{max} = \alpha_1 \cdot \beta_w \cdot f_t$	$\alpha_1 = 1.5$

Figure 5. The geometry of finite element model.

analyzed in the computer in order to verify and establish the accuracy of the modeling strategies. Test layout and material properties for each experiment are given in Figure 6 and Table 4. All the details of Test Case-1 and Test Case-2 can be found Arduini et al. (1997) and Benjeddou et al. (2007), respectively. All the beams are tested under four point load conditions.

Employing the aforementioned modeling strategies, numerical models are reproduced in the computer and load-deflection curves for strengthened RC beams are plotted. Models are seeded with different mesh densities to investigate the mesh sensitivity of each model. For this purpose, three different mesh models are created to represent finer, medium and coarse mesh.

It is clear that the finite element simulation is very capable of capturing the experimentally observed loading trends and magnitudes for the entire loading range. For the Test Case-1, model with medium mesh capture the test result better than the model with finer and course mesh (Figure 7a). The best result is obtained with 50 mm mesh (M50) dimension. However model with finer mesh (M25) give best results in Test Case-2 (Figure 7b). These results show that proposed numerical model is mesh sensitive and proper mesh dimensions should be

investigated carefully.

Table 5 compares the experimental yield loads and deflections with those obtained from the finite element analysis for two test cases. Since the results are almost the same, the proposed finite element model proves its capability to accurately predict the load–deflection relationships of the FRP-strengthened RC beams.

Strain values were only available for Test Case-1. When these values are also compared with those from FEM, very good agreement is caught as plotted in Figure 8.

Effect of FRP bond length on load carrying capacity of strengthened beams

Here, the effect of FRP bond length on the failure load is investigated with verified numerical models. Both in Test Case-1 and Test Case-2, FRP length is changed with the value of L_c/L_f. This ratio is changed between one and five and results are presented with load-deflection curves. Figure 9 shows the parametric study notations of FRP-strengthened RC beams.

For parametric study scheme, eight numerical beams are created with different FRP bond length. Parametric study matrix for both test cases is tabulated in Table 6. In each cases, one beam is bonded along the full length of its soffit ($L_f = L_c$). For keeping FRP bond length within the shear span of the beams L_c/L_f ratio is changed as 1.5, 2, and 2.5. Also one beam in each case is bonded with full length of their constant bending moment region. FRP bond length stays within the constant moment region for beams with L_c/L_f value of 4.5 and 5. Real experimental cases are also shown in Table 6.

Ultimate load capacity of each case (P_u) is divided by that obtained from the model including FRP bonded along the full length of its soffit ($P_{full\ length}$) and results are tabulated in Table 7. Load deflection curves for all these numerical models are also given in Figure 10. Also experimental results of beams without FRP are also included. Both cases show that decreasing the bond length of FRP also decrease the value of ultimate load capacity.

Results clearly indicate that having FRP in the tension face of RC beam has increased the stiffness and the ultimate load capacity of the beam. This is more significant for beams that have FRP in their shear span. When FRP bond length is limited within the constant moment region, change in the load-deflection curve is not that distinct. Also these can be observed from Table 7. As the FRP bond length shortens, the ultimate load capacity also decreases. $P_u/P_{full\ length}$ almost remains constant in constant moment region.

Conclusion

The behavior of reinforced concrete beams strengthened

Table 3. Finite element types employed in numerical modeling.

Element	Code	Description	Additional information
Concrete	CPE4R	Four-noded plain strain	Reduced integration
Steel	T2D2	Two-noded truss	Embedded to concrete
Epoxy	COH2D4	Four-noded solid element	Two dimensional cohesive element
FRP	CPS4R	Four-noded plain stress	Reduced integration
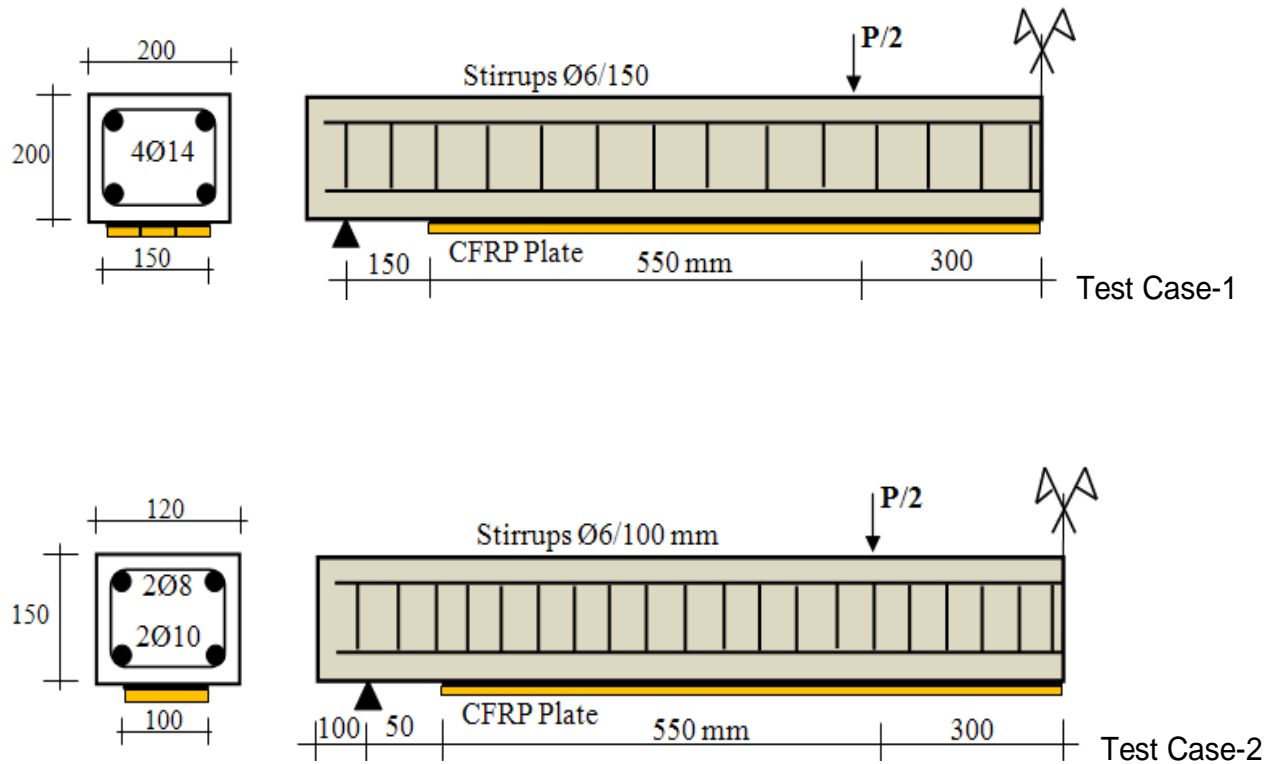
Figure 6. Layout of test beam (dimensions are mm).

Table 4. Material properties of test beams.

Test case	Beam reference name	Concrete			CFRP plate			Epoxy		Steel
		E (GPa)	f_c' (MPa)	f_t (MPa)	E (GPa)	f_t (MPa)	t_f (mm)	E (GPa)	f_t (MPa)	f_y(MPa)
1	A3	25	33	2.6	167	2906	1.3	11	26	540
2	RB1	30	21	1.86	165	2800	1.2	12.8	4	400

with FRP is simulated using the proposed finite element method. The effect of different bond length is evaluated. Modeling steps regarding the nonlinear analysis are explained to create a two dimensional finite element model. Conclusions derived from this study are as follows:

The FEM models are capable of predicting the load–deflection behavior of FRP-strengthened RC beams. The ratios of predicted and experimental maximum loads along with displacements are in acceptable range. However, mesh sensitivity needs to be investigated for each model.

Results from numerical analysis indicate that FRP bond length is very important to obtain satisfactory strengthening targets. The load carrying capacity of the beams decreases rapidly when the bond length distance shortens.
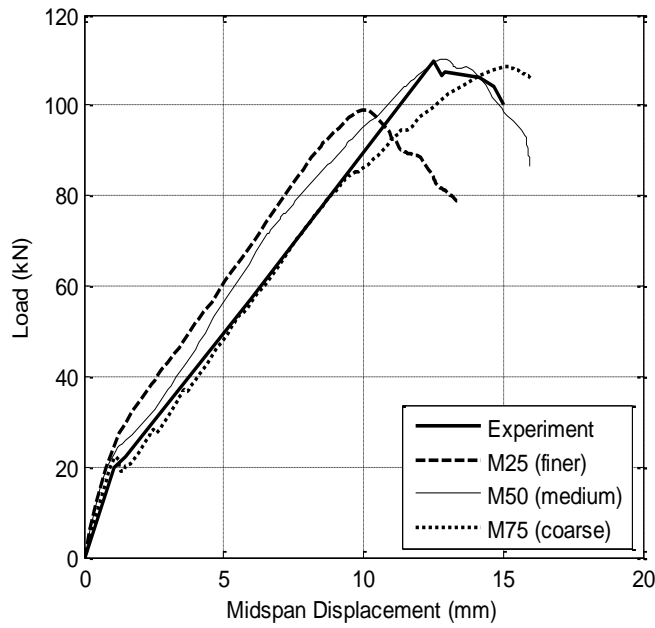
a) Test Case-1
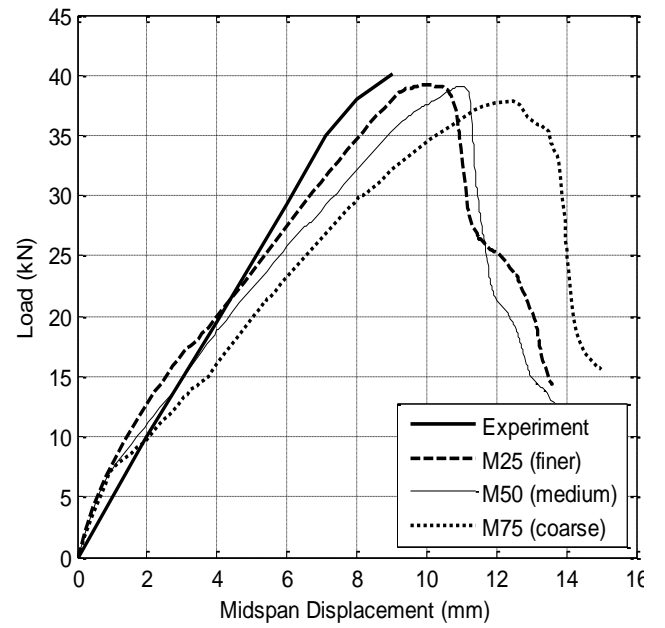
b) Test Case-2

Figure 7. Results obtained from mesh sensitivity study.

Table 5. Comparison of test results.

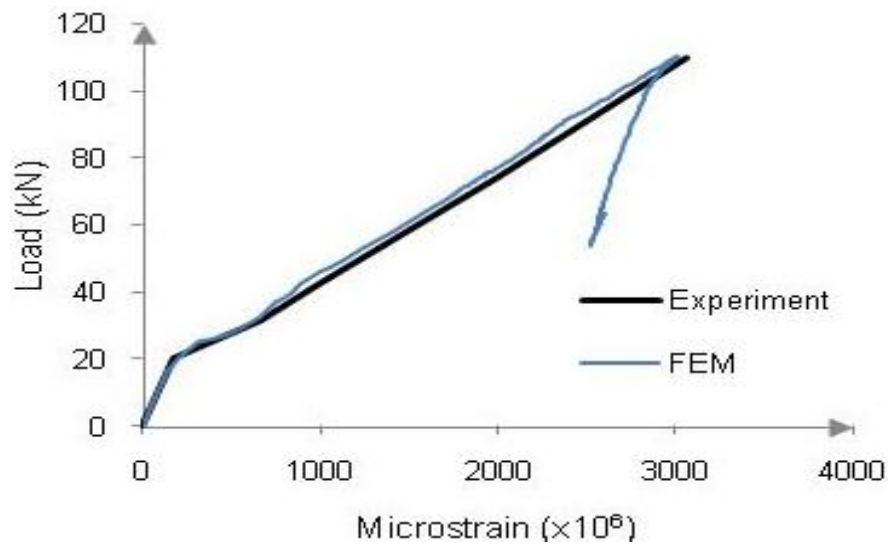| Test	Test Case 1		Test Case 2	
	Yield load (kN)	Deflection (mm)	Yield load (kN)	Deflection (mm)
Experiment	109.89	12.48	40.11	9.02
Finite element	109.83	12.64	39.20	9.96
Num./Exp.	0.99	1.01	0.97	1.10

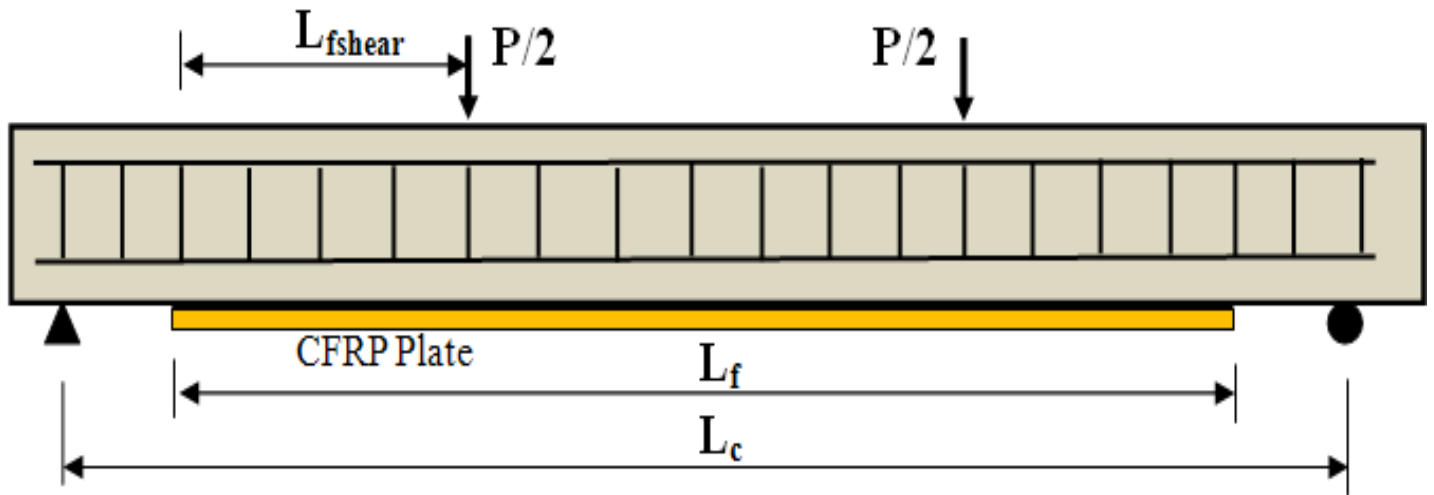**Figure 8.** Comparison of midspan FRP strain for experimental and FEM results.

Figure 9. Parametric study notations of FRP-strengthened beam.

Table 6. Parametric study matrix.

Test	Test Case-1			Test Case-1		
Region where FRP extents	$L_c=2000$			$L_c=1800$		
	L_f	L_{fshear}	L_c/L_f	L_f	L_{fshear}	L_c/L_f
Full length	2000	700	1	1800	600	1
Experiment	1700	550	1.17	1700	550	1.06
Shear span	1333	367	1.5	1200	300	1.5
Shear span	1000	200	2	900	150	2
Shear span	800	100	2.5	720	60	2.5
Constant moment	600	0	3.33	600	0	3
Constant moment	444	0	4.5	400	0	4.5
Constant moment	400	0	5	360	0	5

Table 7. Ultimate load capacity of numerical models

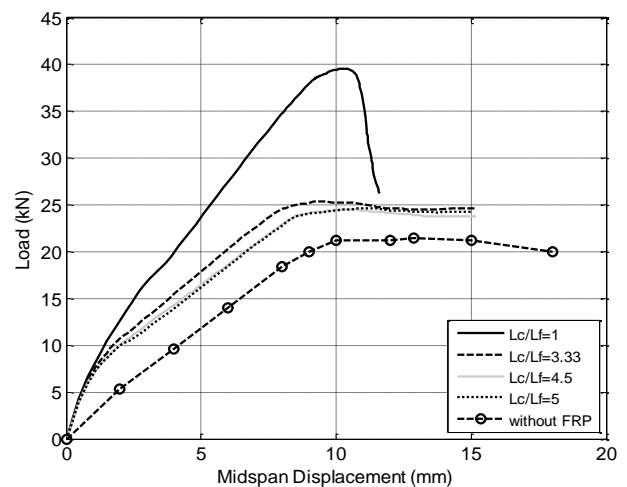| Test Case-1			Test Case-2		
L_c/L_f	P_u	$P_u/P_{full\ length}$	L_c/L_f	P_u	$P_u/P_{full\ length}$
1	108.57	1.00	1	39.53	1.00
1.17	110.32	1.02	1.06	39.20	0.99
1.5	98.5	0.91	1.5	30.80	0.78
2	87.3	0.80	2	26.32	0.67
2.5	80.14	0.74	2.5	25.60	0.65
3.33	76.07	0.70	3	25.37	0.64
4.5	73.35	0.68	4.5	24.47	0.62
5	71.53	0.66	5	24.39	0.62
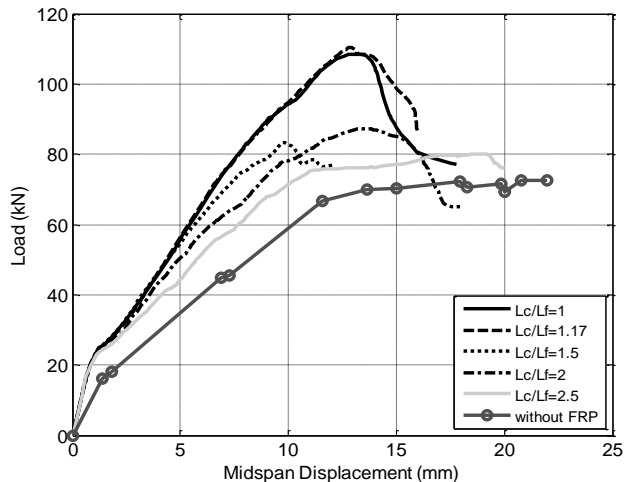
a) Load-deflection responses of Test Case-1 beams (FRP bond length extends to shear span)
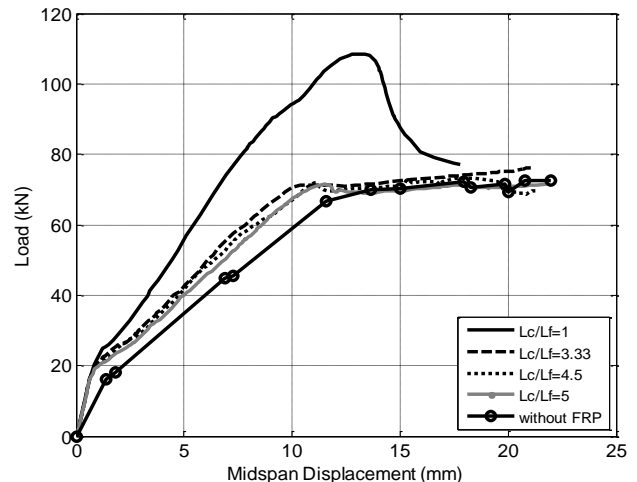
b) Load-deflection responses of Test Case-1 beams (FRP bond length stays in constant moment region)
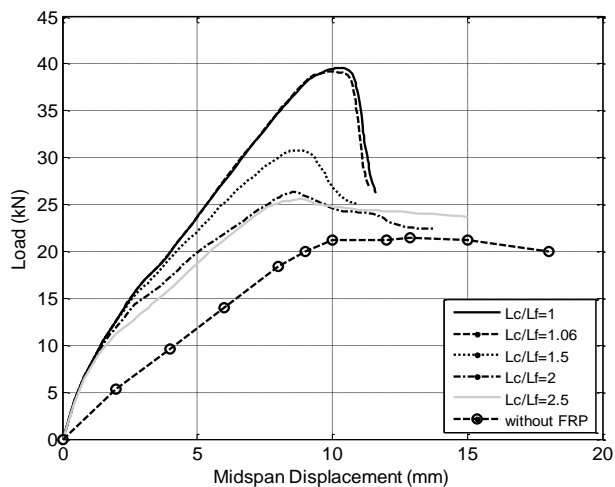
c) Load-deflection responses of Test Case-2 beams (FRP bondlength extends to shear span)

d) Load-deflection responses of Test Case-2 beams (FRP bond length stays in constant moment region)

Figure 10. Effect of FRP bond length on load-midspan displacement response.

REFERENCES

Abaqus (2009). User's Manual, Version 6.9. Hibbit, Karlsson & Sorensen, Inc., Pawtucket, Rhode Island, USA.

Arduini M, Di Tommaso A, Nanni A (1997). Brittle failure in FRP plate and sheet bonded beams. ACI Structural Journal. 94(4): 363-370.

Baky HA, Ebead UA, Neale KW (2007). Flexural and interfacial behavior of FRP strengthened reinforced concrete beams. J. Composites Construct., 11(6): 629-638.

Benjeddou O, Ouezdou BM, Bedday A (2007). Damaged RC beams repaired by bonding of CFRP laminates. Construct. Build. Materials, 21(6): 1301-1310.

CEB-FIP MC90 (1993). Comite Euro-International du Beton, CEB-FIP Model Code 1990. Bulletin D'Information. No: 215, Lausanne.

Coronado AC, Lopez MM (2006). Sensitivity analysis of reinforced concrete beams strengthened with FRP laminates. Cement Concrete Composit., 28(1): 102-114.

Ebead UA, Neale KW, Bizindavyi L (2004). On the interfacial mechanics of FRP-strengthened concrete structures. FRP composites in civil engineering-CICE 2004. pp. 351–359.

Ehsani MR, Saadatmanesh H (1990). Fiber composite plates for strengthening bridge beams. Compos. Struct., 15(4): 343–355.

Hillerborg A, Modeer M, Petersson PE (1976). Analysis of crack formation and crack growth in concrete by means of fracture mechanics and finite elements. Cement Concrete Res., 6: 773–782.

Hognestad E (1951). A study of combined bending and axial load in reinforced concrete members. University of Illinois Engineering, Exp. Sta. Bull., No: 399.

Lu XZ, Ye LP, Teng JG, Ye LP, Jiang JJ (2005). Bond-slip models for FRP sheets/plates bonded to concrete. Eng. Struct., 27(6): 920-937.

Malek A, Saadatmanesh H (1998). Analytical study of reinforced concrete beams strengthened with web-bonded fiber-reinforced plastic plates or fabrics. ACI Structural J. 95(3): 343–352.

Nitereka C, Neale KW (1999). Analysis of reinforced concrete beams strengthened in flexure with composite laminates. Canadian J. Civil Eng., 26(5): 646–654.

Niu H, Karbhari VM, Zhishen W (2006). Diagonal macro-crack induced debonding mechanisms in FRP rehabilitated concrete. Compos. Part B: Eng., 37: 627-641.

Pham H, Al-Mahaidi R (2005). Experimental and finite element analysis

of RC beams retrofitted with CFRP fabrics. ACI Special Publications. 230: 499-514.

Rots JG (1988). Computational modeling of concrete fracture. PhD Thesis, Delft University of Technology, Netherlands.

Sumer Y, Aktaş M (2010). Defining parameters for concrete damage plasticity model. 9th International Congress on Advances in Civil Engineering. Trabzon, Turkey.

Takahashi Y, Sato Y, Ueda T, Maeda T, Kobayashi A (1997). Flexural behavior of RC beams with externally bonded carbon fiber sheet. Nonmetallic (FRP) reinforcement for concrete structures, Japan Concrete Inst., 1: 327–334.

Yang H, Wu ZS, Yoshizawa H (2001). Theoretical solutions on interfacial stress transfer of externally bonded steel/composite laminates. J. Struct. Mechanics Earthquake Eng., JSCE. 18(1): 27–39.

Yang Z, Chen J, Proverbs D (2003). Finite-element modeling of concrete cover separation failure in FRP plated RC beams. Construct. Build. Materials. 17(1): 3–13.

Yu T, Teng JG, Wong YL, Dong SL (2010). Finite element modeling of confined concrete-II: Plastic-damage model. Eng. Struct., 32(3): 680-691.